Performance Comparison of R1234yf and R134a in a Heat Pump: A Simulation-Based Assessment Using Aspen Plus

Ramya B N[1] , Vinayak B Hemadri[2*]

[1] Department of Mechanical Engineering, Dayananda Sagar University, Bangalore, Karnataka, India

*Corresponding author: vinayak-me@dsu.edu.in

Abstract. Heat pumps (HPs) are increasingly recognized as energy-efficient and environmentally sustainable solutions for heating applications. The selection of refrigerant plays a critical role in determining both the thermodynamic performance and environmental impact of HP systems. This study presents a comparative simulation-based analysis of two refrigerants—R1234yf (a hydrofluoroolefin with ultra-low global warming potential, GWP ≈ 1) and R134a (a widely used hydrofluorocarbon with GWP = 1300)—in a heat pump cycle modeled in Aspen Plus. The system is evaluated under two process water inlet temperature scenarios (35 °C and 45 °C), with a constant domestic hot water output requirement of 60 °C. Simulation results show that R134a consistently achieves higher coefficients of performance (COPs ranging from 6.05 to 8.52) compared to R1234yf (COPs from 5.09 to 7.01), primarily due to its higher latent heat of vaporization and lower compression work. However, R1234yf offers a compelling environmental advantage with negligible GWP. The findings highlight a clear trade-off between energy efficiency and environmental sustainability, providing practical insights for refrigerant selection in heat pump design. The validated simulation workflow also offers a reproducible framework for rapid screening of alternative refrigerants in early-stage system development.

Keywords: Heat pump, refrigerant, coefficient of performance, thermodynamic performance, Global warming potential

List of Abbreviations

COP: Coefficient of Performance
EoS: Equation of State
GWP: Global Warming Potential
HC: Hydrocarbon
HFC: Hydrofluorocarbon
HFO: Hydrofluoroolefin
HP: Heat Pump
ODP: Ozone Depletion Potential
p-h diagram: Pressure–Enthalpy diagram
REFPROP: Reference fluid Properties

List of Symbols

Cp: specific heat capacity at constant pressure, kJ/(kg·K)
h: enthalpy, kJ/kg

V. Kumar et al. (eds.), *Proceedings of the International Conference on Advanced Design, Manufacturing, and Sustainable Energy Systems (ICADMSES 2026)*, Atlantis Highlights in Engineering 45,
https://doi.org/10.2991/978-94-6239-750-7_38

k: thermal conductivity, W/(m·K)
$\dot{m}$: mass flow, kg/s
P: pressure, bar
P_r: reduced pressure, –
Pr: prandtl number, –
Q: heat flow, kW
T: temperature, °C
W: compressor power input (work input), kW
ρ: density, kg/m^3
μ: dynamic viscosity, μPa·s
σ: surface tension, mN/m

List of subscripts

c: condensation
cr: critical
e: evaporation
l: liquid
nor: normal
r: reduced
R: refrigerant
sat: saturated
v: vapor

1 Introduction

Heat pumps (HPs) have been a well-established technology for many years and are now widely used for heating and cooling in a variety of buildings—such as apartments, shops, hospitals, and office complexes—due to their comparatively high energy efficiency.

HPs can be regarded as part of environmentally friendly technologies that utilize renewable energy sources. Currently, HP technology is rapidly advancing worldwide as a clean and energy-efficient solution for heating and air conditioning. Depending on the heat source, HPs are classified as water-source, air-source, or ground-source systems [1].

A key consideration in HP design is the choice of refrigerant, as it significantly affects the system's efficiency, heating capacity, and operational range [2]. Refrigerants used in vapor compression cycles are increasingly governed by stringent regulations that limit their environmental impact—particularly their global warming potential (GWP) and ozone depletion potential (ODP)—as well as safety requirements related to flammability. Consequently, the search continues for alternative refrigerants that not only comply with evolving regulatory standards but also enable technically viable, efficient, and safe operation [3].

Current research efforts are primarily directed toward natural refrigerants—especially hydrocarbons (HCs)—and hydrofluoroolefins (HFOs) as substitutes for conventional hydrofluorocarbons (HFCs) across various applications, owing to their low GWP and alignment with environmental regulations [4-7]. Zilio et al. [8] experimentally evaluate R1234yf (HFO) as a replacement for R134a (HFC) in automotive air conditioning systems. Sanchez et al. [9] assess five low-GWP alternatives—R290 (HC), R600a (HC), R1234yf, R1234ze(E) (HFO), and R152a (HFC)—for refrigeration and air-conditioning applications in place of R134a. Rasti et al. [10] examine R600a as a substitute for R134a in domestic refrigerators.

While numerous experimental studies have been published comparing the performance of different refrigerants, such investigations are often time-consuming and costly, requiring specialized equipment, extensive instrumentation, and significant resources. To address this challenge and enable rapid, cost-effective screening of alternative refrigerants, simulation-based approaches offer a powerful complement to experimental work.

This study presents a performance comparison of a HP operating with R1234yf and R134a using the process simulation software Aspen Plus. The work not only evaluates the thermodynamic and efficiency differences between the two refrigerants under comparable operating conditions but also provides a structured, reproducible workflow for simulating HP cycles with various working fluids. This methodology supports early-stage refrigerant screening and system optimization, facilitating the transition toward environmentally sustainable and technically robust HP solutions.

2 Working principle of heat pumps

Fig. 1 illustrates the four essential components of a standard HP. The system operates in a closed loop, comprising four primary components: the compressor, condenser, expansion valve, and evaporator. The process begins at the compressor. Its primary function is to draw in low-pressure, low-temperature refrigerant vapor from the evaporator and compress it, significantly increasing its pressure and temperature. This high-pressure, superheated gas then flows to the condenser. Here, the refrigerant releases its thermal energy to the surrounding environment (e.g., indoor air or water for space heating). As it loses heat, the refrigerant condenses from a gas into a high-pressure liquid. Next, this high-pressure liquid passes through the expansion valve. This device acts as a restriction, causing a rapid drop in the refrigerant's pressure and temperature. As the refrigerant exits the valve, it becomes a low-pressure, low-temperature mixture of liquid and vapor. Finally, this cool mixture enters the evaporator. Here, the refrigerant absorbs thermal energy from the external environment (typically outdoor air, ground water, or process water). This heat absorption causes the refrigerant to boil and evaporate back into a low-pressure vapor. The cycle then repeats as the low-pressure vapor returns to the compressor to be compressed again.

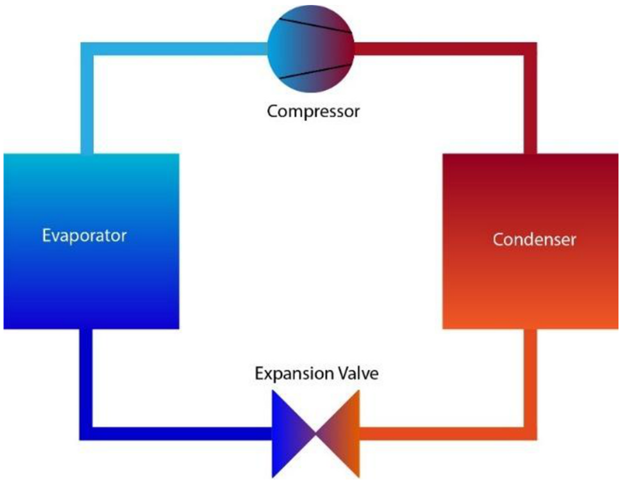

Fig. 1. Basic Schematic of a heat pump cycle.

Fig. 2 plots a HP cycle on pressure-enthalpy diagram. During compression (1-2), the refrigerant vapor is adiabatically compressed. Its pressure rises, and consequently, its temperature also increases. The enthalpy of the refrigerant increases due to the work input from the compressor. The compression work (W) can be calculated by:

$$W = \dot{m}_R(h_2 - h_1) \quad (1)$$

where $\dot{m}_R$ is the refrigerant mass flow, h_2 is the specific enthalpy of refrigerant at point 2, and h_1 is the specific enthalpy of refrigerant at point 1.

The refrigerant exits the compressor at point 2 as a superheated vapor. Next, the superheated vapor enters the condensation process (2-3). At constant pressure, the refrigerant releases its thermal energy to the heating system. Enthalpy decreases as heat is rejected. The useful heat output from the condenser (Q_c) is given by:

$$Q_c = \dot{m}_R(h_3 - h_2) \qquad (2)$$

The expansion takes place from point 3 to 4. The high-pressure liquid refrigerant passes through an expansion valve. This is an isenthalpic process. The pressure and temperature of the refrigerant drop abruptly as

it passes through the valve. At the end of this process (point 4), the refrigerant is a low-pressure, low-temperature mixture of liquid and vapor. Finally, the cycle completes as the refrigerant moves from point 4 back to point 1. This is the evaporation process, occurring at a constant pressure. The refrigerant absorbs heat from the low-temperature source, causing the remaining liquid to fully vaporize. The evaporation heat input (Q_e) can be determined by:

$$Q_e = \dot{m}_R(h_1 - h_4) \qquad (3)$$

This heat absorption is the useful effect of the HP, providing heating to the desired space. The cycle then repeats, continuously transferring thermal energy from a cooler reservoir to a warmer one, powered by the mechanical work input during compression. The difference between the heat rejected in the condenser and the heat absorbed in the evaporator represents the net work input required to drive the cycle. A larger difference generally indicates higher work input, while the position and shape of the cycle are influenced by the operating temperatures and the properties of the refrigerant used. The performance of the HP is often measured by its Coefficient of Performance (COP):

$$COP = \frac{Q_c}{W} \qquad (4)$$

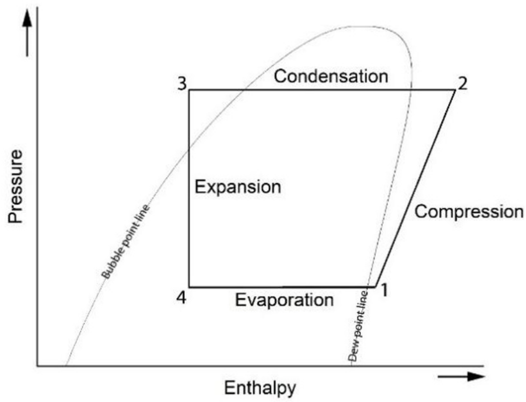

Fig. 2. p-h diagram of heat pump cycle.

3 Refrigerants

The working fluid must possess a reliable thermodynamic property model, besides meeting environmental, safety, and stability criteria, including GWP, ODP, toxicity, flammability, material compatibility [19,20]. This study evaluates two refrigerants: R1234yf and R134a. Although R134a is efficient, non-flammable, and widely used, its high GWP has driven the adoption of lower-impact alternatives such as R1234yf [11], which offers a significantly reduced environmental footprint [12]. Table 1 summarizes key thermophysical properties of both refrigerants at 25 °C. In terms of thermodynamic properties, the normal boiling temperature (T_{nor}) of R1234yf is −29.48 °C, slightly lower than that of R134a (−26.1 °C). Both refrigerants exhibit similar saturation pressures (P_{sat}) at 25°C, with R1234yf showing a slightly higher value. However, R134a has a slightly higher critical temperature (101.1 °C vs. 94.3 °C) and critical pressure (40.6 bar vs. 33.8 bar), suggesting a marginally broader operational range for R134a. R134a possesses a substantially higher enthalpy of vaporization (h_e), meaning it can absorb more heat per kilogram during the evaporation phase compared to R1234yf. This can influence the required mass flow rate and overall system efficiency. The specific heat capacities at constant pressure (C_p) in both liquid and vapor phases are very close. The transport properties reveal further distinctions. R1234yf has a lower liquid density (ρ_l), liquid dynamic viscosity (μ_l), surface tension (σ) and liquid thermal conductivity (k_l) than R134a. Lower viscosity and surface tension generally promote better flow characteristics and potentially enhance heat transfer. Conversely, lower thermal conductivity could be a disadvantage for heat conduction. The vapor phase thermal conductivities (k_v), however, are nearly identical. Finally, the Prandtl numbers (Pr), which relate momentum diffusivity to thermal diffusivity, are very similar for both refrigerants. This suggests that their convective heat transfer behavior might be comparable.

Table 1. Properties of R1234yf and R134a at 25 °C [13, 14].

Property	1234yf	R134a
GWP (-)	1zzzzz	1300
T_{nor} (°C)	-29.48	-26.1
T_{cr} (°C)	94.3	101.1
P_{cr} (bar)	33.8	40.6
σ (mN/m)	6.17	8.03
h_e (kJ/kg)	145.4	177.8
k_l (W/m.K)	0.0635	0.0811
k_v (W/m.K)	0.0139	0.0138
C_{pl} (kJ/kg.K)	1.392	1.425
C_{pv} (kJ/kg.K)	1.053	1.032
ρ_l (kJ/m³)	1092	1207
ρ_v (kJ/m³)	37.92	32.35
μ_l (µPas)	152.9	194.9
μ_v (µPas)	11.4	11.7
Pr_l (-)	3.35	3.42
Pr_v (-)	0.868	0.873

4 Methodology

The HP cycle is simulated using Aspen Plus, a comprehensive process simulation platform widely employed in the chemical and process industries. Aspen Plus provides an extensive thermophysical property database, a modular architecture, and robust capabilities for defining components, selecting thermodynamic property methods, and implementing equations of state.

Fig. 3 presents the Aspen Plus model developed in this study to simulate the HP cycle. The primary heat source is process water, which enters the evaporator (Stream P-W-IN). Within this component, the refrigerant absorbs thermal energy from the process water, causing it to evaporate at a low pressure and become superheated by 2 °C. The resulting superheated gaseous refrigerant (Stream 1) is then compressed, resulting in a high-pressure, high-temperature superheated vapor (Stream 2). This high-energy vapor then flows into the condenser.

The condenser is the central heat delivery point of the system. Here, the refrigerant cools and condenses, releasing both sensible and latent heat. This useful heat is transferred to a stream of domestic water, raising its temperature from an inlet of 20 °C (Stream D-W-IN) to a required outlet of 60 °C (Stream D-W-IN). The condensation occurs with a minimum temperature approach of 5 °C. This dictates that the temperature of Stream 2 must be at least 65 °C to effectively heat the domestic water to its target of 60 °C. Finally, the high-pressure liquid refrigerant (Stream 3) passes through the expansion valve, where it undergoes throttling to return to a low-pressure, low-temperature two-phase state (Stream 4), ready to re-enter the evaporator and repeat the cycle.

The system's performance is evaluated using R1234yf and R134a under two distinct scenarios for the process water heat source. In the first scenario, the process water is available at a relatively high inlet temperature of 45 °C with a temperature drop of 5 °C across the evaporator. In the second scenario, the inlet temperature is lower, at 35 °C, with the same 5 °C temperature drop.

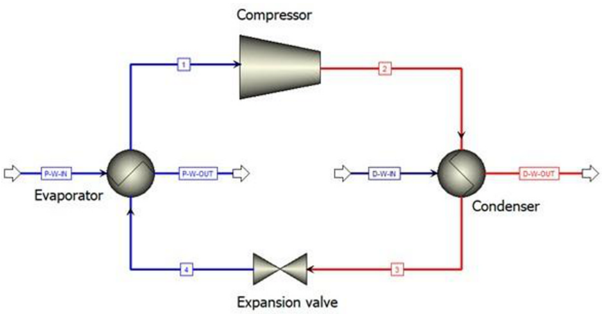

Fig. 3. Simulation model for heat pump with Aspen Plus.

For all simulations, REFerence fluid PROPerties (REFPROP) model is used as property model. This model, developed by the National Institute of Standards and Technology, integrates a Helmholtz-energy-explicit equation of state (EoS), a modified Benedict–Webb–Rubin EoS, and an extended corresponding states model [15]. It is especially well-suited for predicting the thermodynamic and transport properties of refrigerants and hydrocarbons [16]. Pressure drops in piping and heat exchangers are neglected, and the compressor is assigned a constant isentropic efficiency of 0.72. Motor efficiency is not included; its incorporation would slightly reduce the calculated coefficient of performance (COP) [17,21]. All simulations are performed using Aspen Plus version 12.

5 Results

5.1 Validation of simulation model

The experimental tests of a heat pump using refrigerants R1234yf and R134a from [18] were re simulated. Table 2 presents the boundary conditions and the corresponding Coefficient of Performance (COP) values reported in [18] alongside those obtained from the Aspen Plus model under identical operating conditions. The Aspen Plus model demonstrates very good agreement with the experimental COP values from [18], with deviations of less than 2% for both R1234yf and R134a. This confirms the model's accuracy and reliability.

Table 2. Comparison of Experimental and Aspen Plus Simulated COP Values for R1234yf and R134a under Identical Operating Conditions.

Refrigerant	**R1234yf**	**R134a**
Pressure at compressor inlet (bar)	3.46	3.24
Superheating at compressor inlet (°C)	9.84	9.94
Condensation pressure (bar)	9.69	9.54
Condensate super cooling (°C)	6.10	6.05
Compressor efficiency (-)	0.639	0.628
COP obtained in Paper (-)	5.21	5.29
COP obtained by the Aspen Plus model (-)	5.31	5.39

5.2 Heat pump performance using R1234yf and R134a.

Table 3 summarizes the simulation results, which reveal significant performance differences under varying process water inlet temperatures and refrigerant types, while maintaining constant domestic hot water production requirements. Figure 4 provides a visual comparison of the performance metrics.

For both refrigerants, COP increases with a higher process water inlet temperature, indicating improved efficiency when the heat source is warmer. However, R134a consistently outperforms R1234yf across all scenarios, achieving COP values between 6.05 and 8.52, compared to 5.09–7.01 for R1234yf.

This superior efficiency of R134a is attributed to its lower compressor power input: at a 35°C process water inlet temperature, R134a requires 27.6 kW, compared to 32.8 kW for R1234yf; at 45°C, the gap widens further, with R134a consuming 19.6 kW versus 23.8 kW for R1234yf.

These differences can be partially explained by the thermophysical properties of the two refrigerants (refer Table 1). While R1234yf has a significantly lower global warming potential (GWP)—making it environmentally favorable—its physical characteristics lead to higher operational demands. Notably, R134a exhibits a higher latent heat of vaporization (177.8 kJ/kg vs. 145.4 kJ/kg for R1234yf). As a result, less refrigerant mass flow is required to deliver the same useful heat output, which directly reduces compressor power consumption. Moreover, the condensation temperature is consistently higher for R1234yf, resulting in a greater temperature lift, a higher compression pressure ratio, and consequently a higher compressor load. Although R134a has a higher vapor density—an advantage for volumetric efficiency in compression—the dominant factors governing compressor work appear to be the combined effects of pressure ratio and required mass flow rate.

In summary, while R1234yf is the preferred environmental choice due to its negligible GWP, R134a demonstrates superior thermodynamic efficiency in this specific heat pump application, yielding lower compressor power consumption and a higher COP. The selection between the two refrigerants therefore involves a trade-off: R134a offers better energy efficiency and potentially lower operating costs, whereas R1234yf aligns more closely with stringent environmental regulations and sustainability goals. Fig.4. Heat Pump Performance Comparison: R1234yf vs. R134a at 35°C and 45°C Process Water Inlet Temperatures

Table 3. Simulated performance metrics of heat pump using R1234yf and R134a refrigerants under varying process water inlet temperatures.

Refrigerant	**R1234yf**		**R134a**	
Process conditions				
Process water inlet temperature (°C)	35	45	35	45
Process water outlet temperature (°C)	30	40	30	40
Domestic water inlet temperature (°C)	20	20	20	20
Domestic water outlet temperature (°C)	60	60	60	60
Domestic water mass flow (kg/h)	3593	3593	3593	3593
Evaporator inlet temperature (°C)	23	33	23	33
Compressor inlet temperature (°C)	25	35	25	35
Compressor inlet pressure (bar)	6.5	8.5	6.3	8.4
Compressor outlet pressure (bar)	16.5	16.7	15.5	15.8
Condenser inlet temperature (°C)	65	65	67.4	65.5
Condensation temperature (°C)	60.2	60.8	56.5	57.2
Expansion valve inlet temperature (°C)	60.2	60.8	56.5	57.2
Expansion valve outlet vapor fraction (°C)	0.37	0.30	0.28	0.22
Refrigerant mass flow (kg/h)	1.43	1.45	1.06	1.09
Compression pressure ratio (-)	2.56	1.97	2.47	1.88
Performance metrics				
Useful heat rate (kW)	166.9	166.9	166.9	166.9
Heat rate from process water (kW)	134.1	143.1	139.3	147.3
Compressor power input (kW)	32.8	23.8	27.6	19.6
COP	5.09	7.01	6.05	8.52

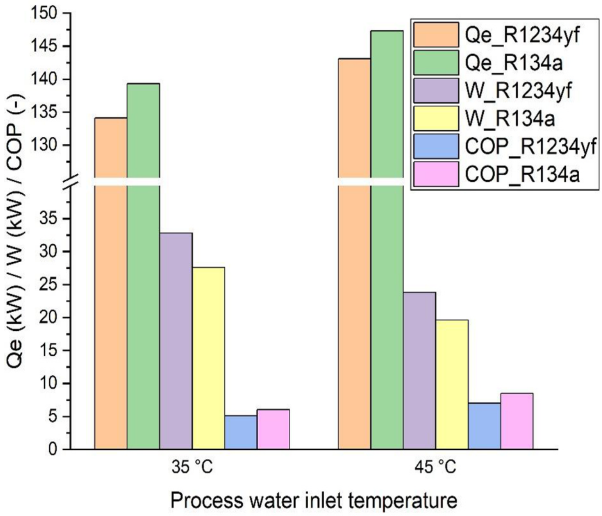

Fig. 4. Performance Comparison of R1234yf and R134a

6 Conclusions

This study demonstrates that while R1234yf represents a significant step forward in reducing the environmental impact of heat pump systems—thanks to its ultra-low GWP—it exhibits lower thermodynamic efficiency compared to the conventional refrigerant R134a under identical operating conditions. The simulations reveal that R134a achieves higher COP values and lower compressor power consumption, largely due to its superior latent heat of vaporization and more favorable pressure-temperature characteristics. Specifically, at a process water inlet temperature of 45 °C, R134a delivers a COP of 8.52, whereas R1234yf reaches only 7.01—a difference of approximately 18%.

Consequently, the choice between R1234yf and R134a involves balancing operational efficiency against regulatory and sustainability goals. For applications where environmental compliance is paramount—such as in regions with strict F-gas regulations—R1234yf remains a viable, albeit less efficient, alternative. Conversely, in contexts prioritizing energy efficiency and lower operating costs, R134a may still be preferable despite its high GWP, especially in systems with closed-loop containment and minimal leakage risk.

The simulation methodology presented here, implemented in Aspen Plus using the REFPROP property package, provides a robust approach for evaluating refrigerant performance in heat pump cycles. This framework can be extended to assess other low-GWP candidates, supporting the accelerated development of sustainable and high-performance heating technologies.

ReferenceS

1. H. Chen, D. Li, and X. Dai, Economic analysis of a wastewater resource heat pump air-conditioning system in North China, Renewable Energy Resources and a Greener Future, 2006.
2. P. A. Domanski, R. Brignoli, J. S. Brown, et al., Low-GWP refrigerants for medium- and high-pressure applications, International Journal of Refrigeration, 2017, pp. 198–209. DOI: https://doi.org/10.1016/j.ijrefrig.2017.08.019
3. C. G. Albà, I. I. I. Alkhatib, F. Llovell, et al., Hunting sustainable refrigerants fulfilling technical, environmental, safety and economic requirements, Renewable and Sustainable Energy Reviews, 2023, Article 113806. DOI: https://doi.org/10.1016/j.rser.2023.113806
4. M. O. McLinden, J. S. Brown, R. Brignoli, et al., Limited options for low-global-warming-potential refrigerants, Nature Communications, 2017, Article 14476. DOI: https://doi.org/10.1038/ncomms14476
5. P. Ganesan and T. M. Eikevik, New zeotropic CO_2-based refrigerant mixtures for cascade high-temperature heat pumps to reach heat sink temperatures up to 180 °C, Energy Conversion and Management: X, 2023, Article 100407. DOI: https://doi.org/10.1016/j.ecmx.2023.100407
6. C. Aprea, F. Ceglia, R. Llopis, et al., Expanded total equivalent warming impact analysis on an experimental standalone fresh-food refrigerator, Energy Conversion and Management: X, 2022, Article 100262. DOI: https://doi.org/10.1016/j.ecmx.2022.100262
7. B. Zühlsdorf, F. Bühler, M. Bantle, et al., Analysis of technologies and potentials for heat pump-based process heat supply above 150 °C, Energy Conversion and Management: X, 2019, Article 100011. DOI: https://doi.org/10.1016/j.ecmx.2019.100011
8. C. Zilio, J. S. Brown, G. Schiochet, et al., The refrigerant R1234yf in air-conditioning systems, Energy, 2011, pp. 6110–6120. DOI: https://doi.org/10.1016/j.energy.2011.08.002
9. D. Sánchez, R. Cabello, R. Llopis, et al., Energy performance evaluation of R1234yf, R1234ze(E), R600a, R290 and R152a as low-GWP R134a alternatives, International Journal of Refrigeration, 2017, pp. 269–282. DOI: https://doi.org/10.1016/j.ijrefrig.2016.09.020
10. M. Rasti, M. S. Hatamipour, S. F. Aghamiri, et al., Enhancement of domestic refrigerator energy efficiency index using a hydrocarbon mixture refrigerant, Measurement, 2012, pp. 1807–1813.
DOI: ttps://doi.org/10.1016/j.measurement.2012.04.002
11. J. J. G. Pabon, A. Khosravi, J. M. Belman-Flores, et al., Applications of refrigerant R1234yf in heating, air conditioning and refrigeration systems: A decade of research, International Journal of Refrigeration, 2020, pp. 104–113. DOI: https://doi.org/10.1016/j.ijrefrig.2020.06.014
12. M. Koban, HFO-1234yf low-GWP refrigerant life cycle climate performance (LCCP) analysis, SAE Technical Paper, 2009.
13. L. Wang, Z. Ding, R. Jiang, et al., Comparative study of flow boiling heat transfer coefficients of R134a, R1234yf, and their mixture (44/56 R134a/R1234yf) in a 3 mm round tube, International Communications in Heat and Mass Transfer, 2026, Article 109993. DOI: https://doi.org/10.1016/j.icheatmasstransfer.2025.109993
14. U. S. Prasad, R. S. Mishra, R. K. Das, et al., Experimental and simulation study of the latest HFC/HFO refrigerants and blends in a vapour compression refrigeration system as alternatives to R134a, Processes, vol. 11, 2023, Article 814. DOI: https://doi.org/10.3390/pr11030814
15. E. W. Lemmon, I. Bell, M. Huber, et al., REFPROP documentation, Release 10.0, National Institute of Standards and Technology (NIST), 2018.
16. AspenTech, Aspen Physical Property System, Aspen Technology Inc., 2006.

17. I. Y. Tirados, Heat pump efficiencies simulated with Aspen HYSYS and Aspen Plus, Master's Thesis, 2015.
18. C. Höges, J. Klingebiel, V. Venzik, et al., Low-GWP refrigerants in heat pumps: An experimental investigation of the influence of an internal heat exchanger, Energy Conversion and Management: X, 2024, Article 100704. DOI: https://doi.org/10.1016/j.ecmx.2024.100704
19. Hemadri, V., P.M.V. Subbarao, Performance assessment and thermodynamic analysis of different organic Rankine cycle (ORC) configurations for IC engine waste heat recovery. Smart Materials and Manufacturing Technologies for Sustainable Development, SME 2025, Sustainable Civil Infrastructures, Springer, Cham, 2026. DOI: 10.1007/978-3-032-05542-2_5
20. Hemadri, V.B., Pubbarao, Thermal integration of reheated organic Rankine cycle (RH-ORC) with gas turbine exhaust for maximum power recovery. Thermal Science and Engineering Progress, 23, 2021, 100876. DOI: ttps://doi.org/10.1016/j.tsep.2021.100876
21. Prashantha, B.G., Narasimham, G.S.V.L., Seetharamu, S., Hemadri, V.B., Theoretical evaluation of stack-based thermoacoustic refrigerators. International Journal of Air-Conditioning and Refrigeration, 30, 2022, 2250008. DOI: https://doi.org/10.1007/s44189-022-00008-2